

Evolutionarily Conserved Multisubunit RBL2/p130 and E2F4 Protein Complex Represses Human Cell Cycle-Dependent Genes in Quiescence

Larisa Litovchick,¹ Subhashini Sadasivam,¹ Laurence Florens,^{2,7} Xiaopeng Zhu,^{3,7} Selene K. Swanson,² Soundarapandian Velmurugan,⁴ Runsheng Chen,³ Michael P. Washburn,² X. Shirley Liu,^{5,6} and James A. DeCaprio^{1,*}

¹Department of Medical Oncology, Dana-Farber Cancer Institute and Department of Medicine, Brigham and Women's Hospital, Harvard Medical School, 44 Binney Street, Boston, MA 02115, USA

²Stowers Institute for Medical Research, 1000 East 50th Street, Kansas City, MO 64110, USA

³Bioinformatics Laboratory, Institute of Biophysics, Chinese Academy of Sciences, Beijing 100101, China

⁴Department of Cancer Biology, Dana-Farber Cancer Institute, Harvard Medical School, 44 Binney Street, Boston, MA 02115, USA

⁵Department of Biostatistics and Computational Biology, Dana-Farber Cancer Institute, 44 Binney Street, Boston, MA 02115, USA

⁶Department of Biostatistics, Harvard School of Public Health, 677 Huntington Avenue, Boston, MA 02115, USA

⁷These authors contributed equally to this work.

*Correspondence: james_decaprio@dfci.harvard.edu

DOI 10.1016/j.molcel.2007.04.015

SUMMARY

The mammalian Retinoblastoma (RB) family including pRB, p107, and p130 represses E2F target genes through mechanisms that are not fully understood. In *D. melanogaster*, RB-dependent repression is mediated in part by the multisubunit protein complex *Drosophila* RBF, E2F, and Myb (dREAM) that contains homologs of the *C. elegans* synthetic multivulva class B (synMuvB) gene products. Using an integrated approach combining proteomics, genomics, and bioinformatic analyses, we identified a p130 complex termed DP, RB-like, E2F, and MuvB (DREAM) that contains mammalian homologs of synMuvB proteins LIN-9, LIN-37, LIN-52, LIN-54, and LIN-53/RBBP4. DREAM bound to more than 800 human promoters in G0 and was required for repression of E2F target genes. In S phase, MuvB proteins dissociated from p130 and formed a distinct submodule that bound MYB. This work reveals an evolutionarily conserved multisubunit protein complex that contains p130 and E2F4, but not pRB, and mediates the repression of cell cycle-dependent genes in quiescence.

INTRODUCTION

Gene expression is regulated by a dynamic assembly of protein complexes as well as specific modifications to DNA and proteins that form chromatin. Control of genes necessary for cell-cycle entry and progression in mamma-

lian cells is dependent, at least in part, on the Retinoblastoma (RB) family of tumor suppressors that includes pRB (RB1), p107 (RBL1), and p130 (RBL2) (Cobrinik, 2005). RB proteins regulate gene expression by interaction with the E2F family of specific DNA-binding transcription factors (reviewed in Dimova and Dyson [2005] and Wikenheiser-Brokamp [2006]). The RB family is thought to inhibit E2F-dependent transcription by sequestering activating E2Fs and recruiting chromatin-modifying factors to E2F-responsive promoters (Frolov and Dyson, 2004).

Genetic knockout studies of RB genes revealed many shared and unique functions for each family member in development, cell-cycle control, and regulation of gene expression (Wikenheiser-Brokamp, 2006). Interestingly, while inactivating mutations in upstream regulators of RB pathway are found in many human cancers, only pRB incurs specific loss-of-function mutations and acts as a bona fide tumor suppressor (Classon and Harlow, 2002; Wikenheiser-Brokamp, 2006). Despite considerable progress, specific roles for p130, p107, and pRB in regulation of gene expression are still far from clear.

Purification of RB homologs from insect cells led to the identification of a multisubunit protein complex that was determined to be essential for silencing of developmentally regulated genes (Korenjak et al., 2004). This complex contained RBF, E2F, DP, and dMyb as well as the previously identified dMyb-interacting proteins Mip120, Mip130, and Mip40 and was referred to as *Drosophila* RBF, E2F, and Myb (dREAM) (Beall et al., 2002; Korenjak et al., 2004). Independently, analysis of Mip120- and Mip130-associated proteins resulted in the identification of a similar complex that also contained Rpd3 (HDAC), L(3)mbt, and Lin-52 (Lewis et al., 2004). Remarkably, *C. elegans* homologs for each of these RBF- and dMyb-associated proteins are products of the synthetic multivulva class B (synMuvB) genes (Ceol et al., 2006; Fay and Han, 2000).

The synMuvB group includes 25 genes (Ceol et al., 2006) and is one of the three genetically linked classes of genes that synthetically function to antagonize Ras signaling in development of the vulva. Recently, the *C. elegans* synMuvB gene products LIN-35/RB, LIN-9, LIN-37/MIP40, LIN-52, LIN-53/RBBP4, LIN-54/MIP120, and DPL-1 were reported to form a complex termed *Dpl-Rb-MuvB* (DRM) similar in composition to the fly dREAM complex (Harrison et al., 2006).

Importantly, homologs of all subunits of the dREAM complex are found in the human genome. Recombinant human Mip120 (LIN54), Mip130 (LIN9), and Mip40 (LIN37) have been reported to bind to a GST-pRB fusion protein (Korenjak et al., 2004), while human LIN9 was shown to interact with pRB and B-MYB (Gagrica et al., 2004; Osterloh et al., 2007; Pilkinton et al., 2006). Using a combination of proteomic, promoter microarray, gene expression, and bioinformatic analyses, we identified and functionally characterized a p130-associated protein complex that represents the human homolog of the fly dREAM and worm DRM and contributes to repression of cell cycle-dependent genes during quiescence.

RESULTS

Human Homologs of dREAM Subunits Interact with p130 and E2F4

To determine whether the human homologs of fly dREAM and worm DRM subunits could form a complex, specific antibodies were generated against the predicted protein sequences of human MuvB-like proteins LIN9 (Gagrica et al., 2004), LIN37, LIN52, and LIN54 (details in the [Supplemental Data](#) available with this article online). Using these antibodies, we detected a reciprocal *in vivo* interaction between MuvB-like proteins in T98G cell extracts (Figure 1A). In addition, all four factors coprecipitated B-MYB while LIN54, LIN9, and LIN37 also bound E2F4 (Figure 1A).

We tested whether specific RB family proteins associate with the MuvB-like proteins. Antibodies against p130 coprecipitated LIN9, LIN37, LIN54 (Figure 1B), and LIN52 (Figure 1C) while the antibodies against pRB or p107 did not. In addition, antibodies against LIN54, LIN9, and LIN37 coprecipitated p130 but were unable to coprecipitate pRB or p107 (Figure 1B). p130 also bound to LIN9, LIN54, and LIN37 in human LF1 primary fibroblast cells (Figure 1D) while pRB did not (Figure S1A). Using a set of deletion mutants of p130, we observed that binding of LIN9 and LIN37 required an intact N terminal as well as the central pocket domains of p130 and was independent of E2F4 binding (Figure S1B). Together, these results imply that the MuvB proteins bind specifically to p130.

Antibodies against LIN52 did not coprecipitate p130 or E2F4 although they coprecipitated LIN9, LIN37, and LIN54 as well as B-MYB (Figure 1A). Conversely, LIN52 was coprecipitated by all other MuvB-like proteins as well as by p130, indicating that LIN52 is a part of human dREAM-like complex. Indeed, we found that V5-tagged LIN52

protein bound to endogenous p130 in anti-V5 immunoprecipitation (IP) (Figure 1E). Therefore, we conclude that p130 and E2F4 associate with a protein complex containing human LIN9, LIN37, LIN52, and LIN54.

Proteomic Analysis Reveals Eight Core Subunits of Human dREAM-like Complex

To determine the composition of the human dREAM-like complex, we combined IP with multidimensional protein identification technology (MudPIT) (Florens and Washburn, 2006). Initially, p130-associated proteins were purified from T98G cells stably expressing HA-tagged human p130 (Litovchick et al., 2004) using an anti-HA antibody. Twelve specifically interacting proteins were detected in at least two of three independent anti-HA IP experiments (Table 1 and Table S1). This result was reproduced using antibodies specific for endogenous p130 (Table S1). Nine out of 12 p130-associated proteins are homologs of the dREAM complex subunits, including E2F4, E2F5, DP1, DP2, LIN9, LIN37, LIN52, LIN54, and RBBP4 (Table 1) (Korenjak et al., 2004; Lewis et al., 2004). In addition, cyclin A, cyclin E2, and CDK2 proteins that have been previously reported to bind to p130 were detected in these experiments (Classon and Dyson, 2001; Payton and Coats, 2002).

We used MudPIT to identify proteins interacting with LIN9, LIN37, and LIN54. Remarkably, IPs with antibodies against LIN9, LIN37, and LIN54 once again resulted in coprecipitation of all subunits of human dREAM-like complex, including p130 (Table 1). No peptides specific for pRB and p107 were detected in any of these IPs (Table S2). Because IP with antibodies against endogenous proteins can interfere with protein-protein interactions, we performed MudPIT analysis of anti-V5 IPs for LIN9-V5 and LIN37-V5 stably expressed in T98G cells. These experiments confirmed binding of human dREAM-like subunits and did not identify any additional interactions (data not shown). The relative abundance of identified peptides in the p130 IPs compared to that observed in the IPs for LIN9, LIN37, and LIN54 indicates that human dREAM-like complex is composed of one stable module containing p130, E2F4/5, and DP1/2 and another module containing the MuvB proteins LIN9, LIN37, LIN52, LIN54, and RBBP4 (Figure S2).

Although MYB was not detected in the p130 IP, peptides specific for MYBL1 (A-MYB) and MYBL2 (B-MYB) were present in IPs for LIN9, LIN37, and LIN54 (Table 1), indicating that these proteins form distinct complexes with either p130 or MYBs. The result that antibodies against LIN52 could coprecipitate other MuvB proteins and B-MYB, but not p130 or E2F4, supports this conclusion (Figures 1A and 1B). Therefore, the human dREAM-like complex differs from the fly complex that contains both RB and Myb (Korenjak et al., 2004; Lewis et al., 2004). Other differences between the fly and human complexes include the lack of L(3)MBT homologs or HDAC1/2 in the latter (Table 1 and data not shown). Although we detected peptides for HDAC3 and other subunits of the

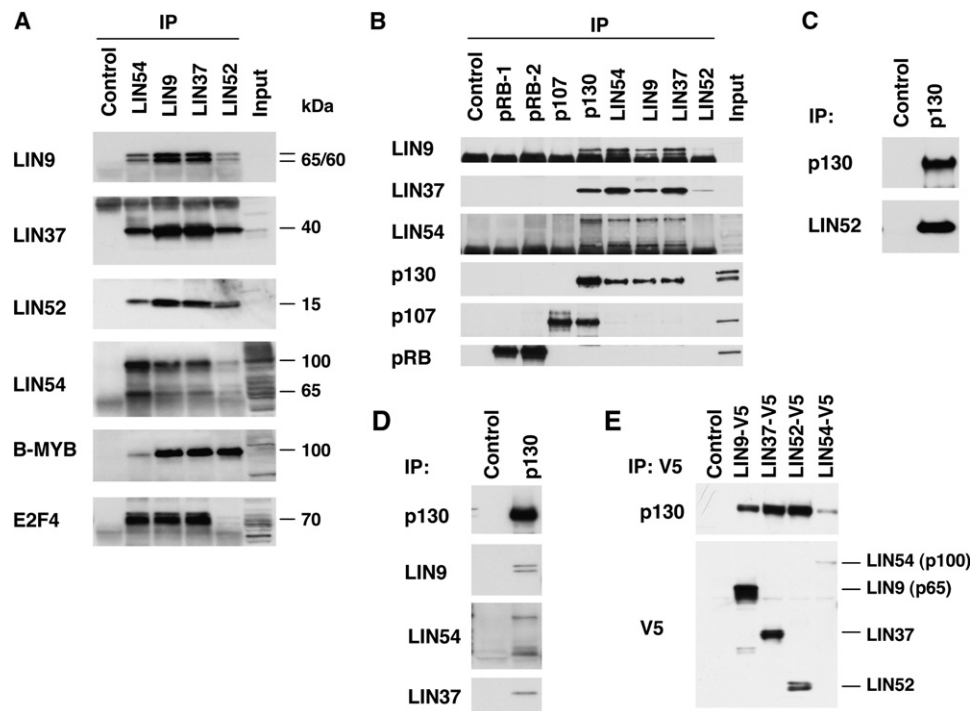


Figure 1. Detection of Human dREAM-like Complex

(A–C) T98G cell extracts were immunoprecipitated with antibodies against indicated proteins or control antibodies. Proteins of interest were detected in the IPs by western blot. Apparent molecular weights including alternatively spliced forms of LIN9 and LIN54 are indicated. p107 protein is present in the p130 IP due to crossreactivity of anti-p130 antibodies with p107.

(D) LF1 cell extracts were immunoprecipitated by anti-p130 or control antibodies, and the indicated proteins were detected in the IPs by western blot.

(E) Extracts from T98G cell lines expressing V5 epitope-tagged LIN9, LIN37, LIN52, or LIN54 and control T98G cells were immunoprecipitated with anti-V5 antibodies, and p130 was detected in the IPs by western blot.

NCoR complex in LIN54 IPs and for SIN3A in LIN37 IPs (Table S2), these proteins were not found in complexes with other subunits or in anti-V5 IPs and were not analyzed further.

These results indicate that human cells contain an evolutionarily conserved complex that we refer to as DP, RB-like, E2F, and MuvB (DREAM), consisting of at least eight subunits, including RBL2/p130, E2F4 or E2F5, DP1 or DP2, RBBP4, LIN9, LIN37, LIN52, and LIN54. We found no evidence that pRB interacts with LIN9, LIN37, or LIN54 subunits of this complex.

DREAM Subunits Bind to E2F Target Promoters in Quiescent Cells

The interaction between p130 and E2F4 is restricted to G0 and the G1 phase of the cell cycle (Cobrinik, 2005). To determine whether the composition of the DREAM complex undergoes changes during the cell cycle, we performed MudPIT analysis of p130 complexes from G0 and S phase cell extracts (Figure 2A and Table S3). The relative abundance of E2F4, DP1, DP2, and other DREAM subunits was increased in p130 IPs from G0 relative to S phase extracts. In contrast, the levels of cyclins A, E1, and E2 as well as CDK2 bound to p130 were increased in S phase

compared to the G0 samples. A coupled IP-western blot assay using extracts prepared from synchronized cells confirmed interaction between p130 and LIN9, LIN37, LIN52, LIN54, and RBBP4 in G0, but not in S phase (Figure 2B and data not shown). This assay also revealed that the MuvB proteins LIN9, LIN37, LIN52, and LIN54 remained associated with each other in S phase and bound B-MYB (Figure 2B and data not shown). Together, these results show that DREAM complex containing p130 and E2F4 exists in quiescent cells and dissociates in S phase when LIN9, LIN37, LIN52, and LIN54 form a subcomplex that binds to B-MYB.

Given that p130 and E2F4 can bind to E2F-dependent promoters in G0 and that the MuvB proteins interact with p130 and E2F4 under these conditions, we hypothesized that the DREAM complex could also bind to E2F target promoters. Using chromatin IP (ChIP) for each DREAM subunit followed by PCR for several known E2F-dependent promoters, we observed that p130, LIN9, LIN54, LIN37, RBBP4, and LIN52 could bind specifically to E2F-dependent promoters (Figure 2C and Figure S3A). Consistent with previous reports that binding of p130 and E2F4 to promoters was restricted to G0/G1 (Balcunaite et al., 2005), we observed that each DREAM subunit had

Table 1. Human DREAM Complex Detected by MudPIT

<i>Drosophila</i>	<i>C. elegans</i>	Human	HAp130 IP	p130 IP	LIN9 IP	LIN37 IP	LIN54 IP
RBF1/2 ^a	Lin-35 ^c	RBL2/p130	172 ^d (26.9) ^e	652 (38.1)	17 (4.9)	62 (19.3)	116 (23.3)
E2F2 ^a	Efl-1 ^c	E2F4	83 (39.2)	85 (35.4)	10 (11.6)	24 (13.4)	61 (41.2)
		E2F5	21 (26.6)	25 (22.8)	0 (0)	0 (0)	4 (12.7)
DP ^a	Dpl-1 ^c	DP1	45 (39.8)	76 (45.1)	6 (12.4)	11 (12.7)	28 (23.4)
		DP2	3 (15.5)	17 (15.8)	1 (7.0)	2 (4.9)	7 (17.1)
p55/Caf1 ^a	Lin-53 ^c	RBBP4	9 (5.6)	55 (59.5)	73 (50.8)	129 (50.8)	52 (20.5)
Mip130 ^a	Lin-9 ^c	LIN9	33 (20.3)	58 (31.2)	162 (34.8)	291 (55.6)	138 (33.7)
Mip40 ^a	Lin-37 ^c	LIN37/LOC55957	8 (20.3)	45 (18.7)	50 (18.7)	182 (47.6)	68 (37.4)
dLin52 ^b	Lin-52 ^c	LIN52/LOC91750	8 (28.4)	20 (31.9)	51 (24.1)	25 (42.2)	33 (42.2)
Mip120 ^a	Lin-54 ^c	LIN54/LOC132660	66 (35.8)	78 (34.8)	79 (22.7)	317 (48.2)	763 (50.3)
Myb ^a	n/a	MYBL2	0 (0)	0 (0)	40 (28.1)	79 (22.7)	9 (11.7)
		MYBL1	0 (0)	0 (0)	2 (4.7)	2 (1.9)	2 (4.7)
Rpd3 ^b	Hda-1	HDAC1/2	0 (0)	0 (0)	0 (0)	0 (0)	0 (0) ^f
L(3)mbt	Lin-61	L3MBTL	0 (0)	0 (0)	0 (0)	0 (0)	0 (0)

^a Detected in both dREAM and Myb-MuvB complexes (Korenjak et al., 2004; Lewis et al., 2004).

^b Detected only in Myb-MuvB complexes (Lewis et al., 2004).

^c Physically interact in *C. elegans* (Harrison et al., 2006).

^d Total number of peptides detected by MudPIT in three experiments.

^e Percent of sequence coverage.

^f Peptides for HDAC3 were detected in one of three LIN54 IPs.

significantly higher ChIP enrichment for the two tested E2F-dependent promoters in G0 phase compared to S phase (Figures 2D and 2E and Figure S3B).

E2F Binding Sites Are Co-Occupied by the Human DREAM Proteins

Previous genome-wide location analysis (ChIP-chip) revealed a significant overlap of regions bound by p130 and E2F4 and identified 287 p130/E2F4 target promoters (Cam et al., 2004). To determine the fraction of E2F4- and p130-bound promoters that were also occupied by the MuvB proteins, we performed ChIP-chip with antibodies against p130, E2F4, LIN9, and LIN54 using chromatin prepared from T98G cells arrested in G0 by serum deprivation and probed a tiled array containing more than 25,000 human promoters. Biological triplicate data for each of the four ChIP-chip factors were analyzed using a model-based analysis of tiling (MAT) array algorithm (details in Experimental Procedures). At p value 10^{-5} (MAT score 5.5), MAT predicted 2451 p130 (false discovery rate [FDR], 2.72%), 2098 E2F4 (FDR, 2.73%), 2735 LIN9 (FDR, 2.19%), and 1861 LIN54 (FDR, 4.11%) binding sites (Figure 3). We identified 954 common targets between E2F4 and p130, which includes ~70% of the previously reported promoters (Cam et al., 2004). This significantly larger number of p130- and E2F4-bound regions than previously reported was probably due to a combined effect of higher sensitivity of the detection method used, increased

promoter microarray coverage, and different analysis algorithm.

Overall, the binding locations and strength of LIN9, LIN54, p130, and E2F4 were significantly correlated. The shared targets between LIN9 and p130, LIN9 and E2F4, and p130 and E2F4 had remarkable MAT score correlation of 0.96, 0.94, and 0.95, respectively (Figure 3). Among all the binding regions identified, 435 were bound by all four factors; 818 were bound by p130, E2F4, and LIN9; and 1699 were bound by at least two factors. Most notably, the 435 regions bound by all four factors constituted the most ChIP-enriched targets. LIN54 bound to fewer promoters than the other factors tested, and the MAT scores for LIN54-bound regions were on average about 2-fold lower than for the other three factors (Table S4). Nevertheless, the regions bound by LIN54 overlapped with those bound by the other factors and displayed a high correlation of binding strength (Figure 3). In the group of 818 targets, the 383 promoters that LIN54 failed to bind were also bound relatively less well by p130, E2F4, and LIN9. The apparent smaller number of LIN54 binding regions and lower correlation with the binding regions of the other three factors might be explained by the slightly lower affinity of the anti-LIN54 antibody. Alternatively, LIN54 may bind indirectly to DNA through the other three cofactors. Overall, this analysis shows that any promoter bound strongly by one of the factors was also likely bound by other factors.

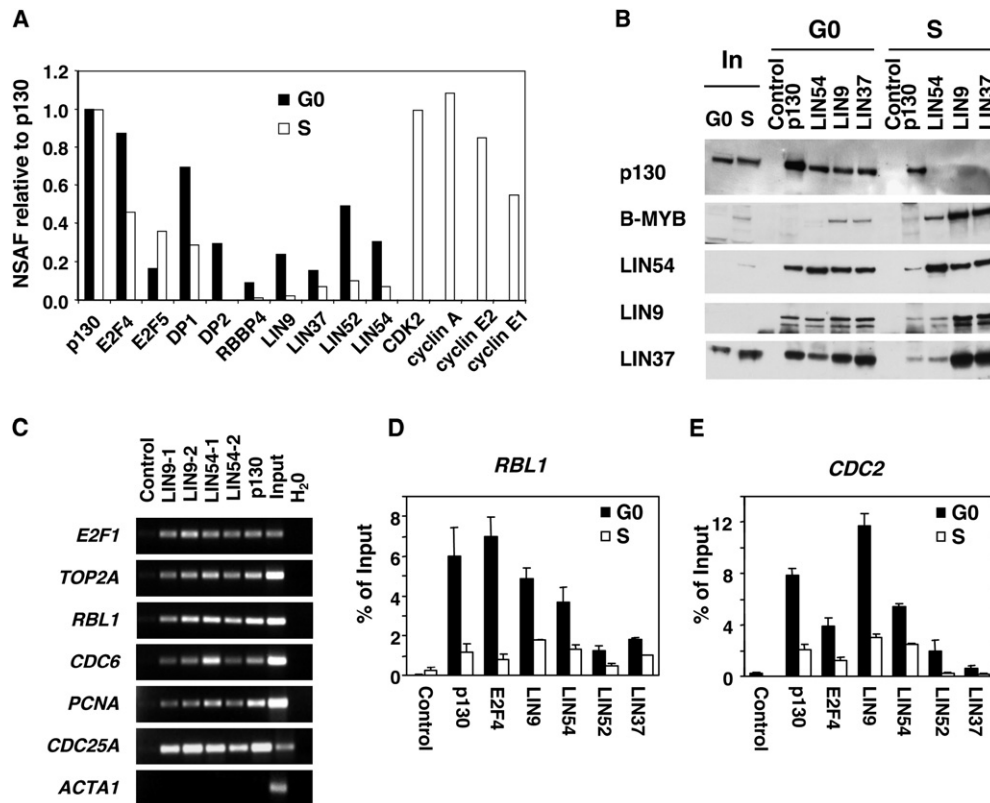


Figure 2. Binding of DREAM Subunits to p130 and to E2F-Dependent Promoters Is Increased in G0

(A) Anti-HA IPs from T98G/HAp130 cells synchronized in G0 and S phase were analyzed by MudPIT (details in Experimental Procedures). Graph shows normalized spectral abundance factors (NSAFs) for interacting proteins (Florens et al., 2006) relative to NSAF p130. A representative of two experiments, each containing the G0 and S phase samples, is shown.

(B) T98G cells were synchronized in G0 and S phase and used to immunoprecipitate indicated DREAM subunits. B-MYB and the DREAM subunits were detected in the cell extracts (Input) and IPs by western blot.

(C) Chromatin was immunoprecipitated with indicated antibodies and PCR amplified to detect E2F4 target promoters. PCR products were analyzed by agarose gel electrophoresis. PCR with input chromatin is shown as a positive control. H₂O is a no-template control.

(D and E) T98G cells were synchronized in G0 and S phase and used for ChIPs with indicated antibodies followed by qPCR to amplify *RBL1* (D), *CDC2* (E), or *ACTA1* (Figure S3B) promoters. Graphs show the amount of DNA present in each of the ChIP samples calculated as percent of the total input chromatin. Average values and standard deviations from three independent experiments are shown.

To determine the regions bound by DREAM complex in S phase, we repeated the ChIP-chip analysis with chromatin prepared from T98G cells synchronized in S phase. We found that each of the factors bound the same regions in S phase as in G0 but with considerably lower efficiency (Table S4 and Figure S4). In addition, we observed a decreased MAT score correlation between the regions bound by any two factors in S phase (Figure S4A). A few targets showed slightly stronger binding in S phase compared to G0, but they had relatively low MAT scores, indicating overall weaker binding (Table S4). To compare occupancy of each DREAM-bound region in G0 and S phase, we generated a heatmap showing the relative ChIP enrichment of regions bound by LIN9, LIN54, p130, and E2F4. The 818 regions bound by p130, E2F4, and LIN9 were ranked by the average MAT score for all experiments and color coded according to the binding strength.

As shown in Figure 4B, the binding strength of all factors for each promoter region was generally higher in G0 compared to S phase. This can be illustrated by the specific binding of each factor to the *CDC6* promoter where the degree of binding of each factor near the first exon is higher for chromatin prepared from G0 cells compared to S phase cells (Figure 5A). The observed S phase DREAM binding to promoters could be due to a delayed G0 to S progression in a fraction of cells. It should be also noted that the ChIP-chip assay itself is only semi-quantitative because it relies on PCR amplification of the chromatin DNA and enzymatic detection of labeled DNA fragments on the promoter microarray. Therefore, our data support the model that the entire DREAM complex dissociates from the target promoters in S phase as was previously shown for p130 and E2F4 (Balciunaite et al., 2005).

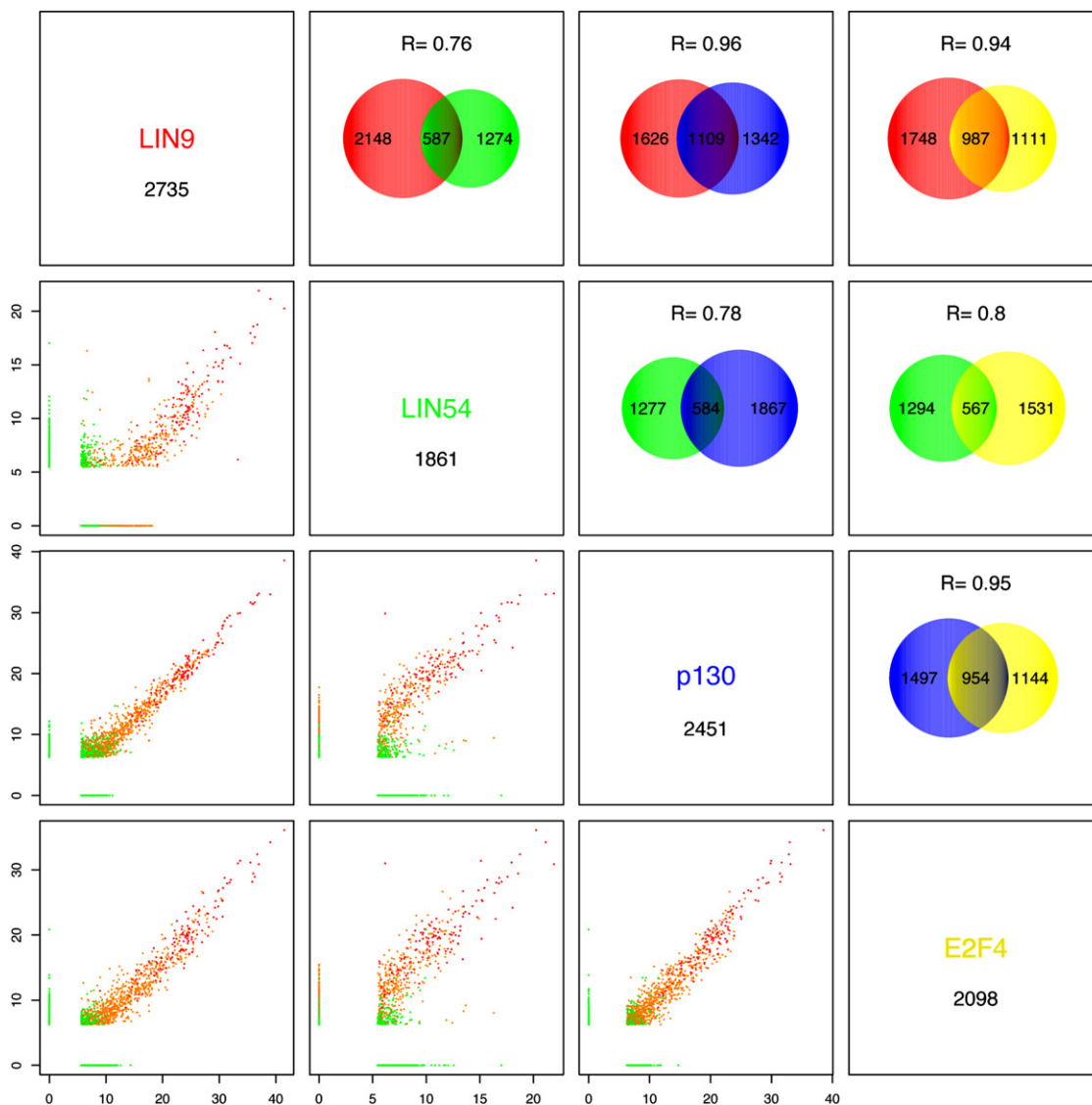


Figure 3. Genome-Wide In Vivo Promoter Binding Sites of LIN9, LIN54, p130, and E2F4 in G0-Arrested Cells Overlap and Are Highly Correlated

The upper right panels display the number of binding sites for each factor and pair-wise overlap in Venn diagrams, with circle size and overlap drawn to scale. The “R” value represents the correlation coefficient of the binding enrichment of the overlapping sites. The lower left panels display the correlation plots of sites bound by each pair of factors. Y axis represents the MAT score of a reported binding site of the factor on the top, and X coordinate represents that of the factor to the right. Sites bound by two factors are shown as green dots, sites bound by LIN9, p130, and E2F4 are shown in orange, and sites bound by all four factors are shown in red.

Given that LIN9 and LIN54 remain bound to each other after cells progress from G0 to S phase, we analyzed 122 regions bound by LIN9 and LIN54 with MAT scores higher than 5 but not bound by p130 or E2F4 (Table S5). We found that these regions were not only bound with relatively low strength but lacked correlation between LIN9 and LIN54 binding (Figure S4B). This indicates that LIN9 and LIN54 do not bind as a complex to promoters after dissociation from p130/E2F4 although it remains possible that either factor interacts individually with DNA or that binding occurs outside the tiled promoter regions.

To determine whether the regions bound by DREAM subunits were enriched for specific DNA sequences, we used an unbiased approach to predict enriched sequence motifs from regions bound by at least two factors in G0 (Ji et al., 2006). This analysis identified E2F, NRF2, CREB, and n-MYC motifs as highly enriched in the bound regions (Figure 4A). The percentage of promoters that contained these motifs decreased with decreasing binding strength (Figure 4A). The E2F binding motif was found in approximately half of the 500 strongest bound promoters and was also significantly enriched when regions bound by

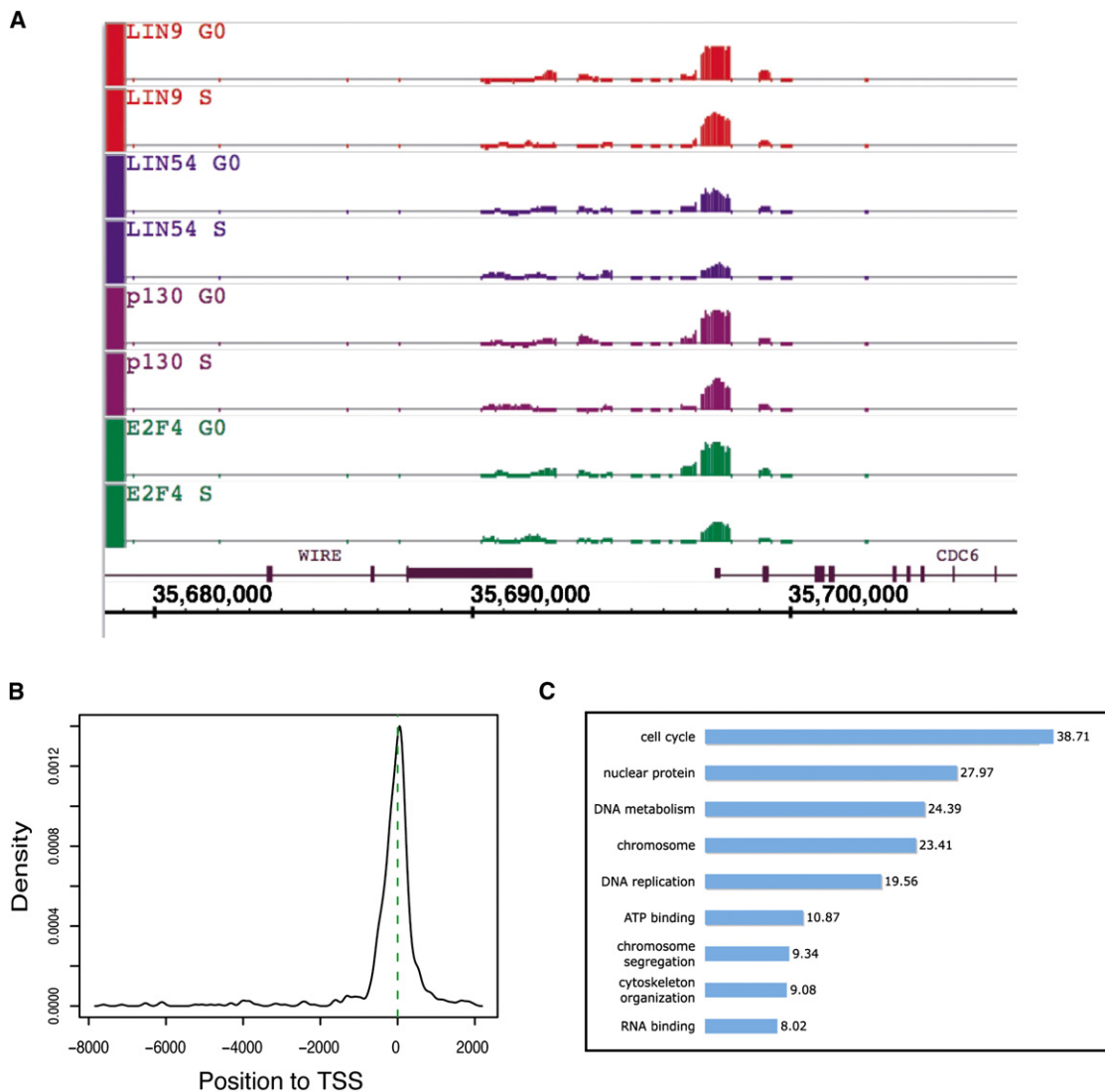


Figure 5. DREAM Complex Binds to the Promoters of Cell Cycle-Related Genes

(A) Representation of MAT scores of all probes along the *CDC6* promoter. Chromosome coordinates of the binding sites and genes are based on Hg18 genome assembly.

(B) Location of the regions bound by p130, E2F4, and LIN9 relative to TSS in G0-arrested cells. "0" indicates TSS, and negative values indicate regions upstream.

(C) The genes bound by p130, E2F4, and LIN9 at their promoters in G0-arrested cells were functionally annotated using the DAVID database (<http://david.abcc.ncifcrf.gov>). Values indicate enrichment score.

of E2F and pocket proteins. While the fly dREAM complex has been implicated in repressing developmentally regulated genes (Dimova et al., 2003; Korenjak et al., 2004), we did not find significant enrichment for this category in our analysis.

DREAM Complex Is a Repressor of Cell Cycle-Dependent Genes

To test whether the DREAM complex promoter binding in G0 is relevant to gene expression, we examined the expression profiles of DREAM target genes. The expression

of a majority of DREAM target genes was significantly higher in cycling cells compared to G0-arrested cells (Figure 6A), and approximately half of the DREAM target genes were upregulated in S phase compared to G0-arrested cells (Figure 6B). The partial induction of DREAM targets in S phase samples could reflect the dynamic activation of cell cycle-dependent genes at several points throughout the G1-to-S transition. Together, the global location and expression analysis data indicate that the presence of the human DREAM complex at promoters in G0 cells correlates with repression of the corresponding

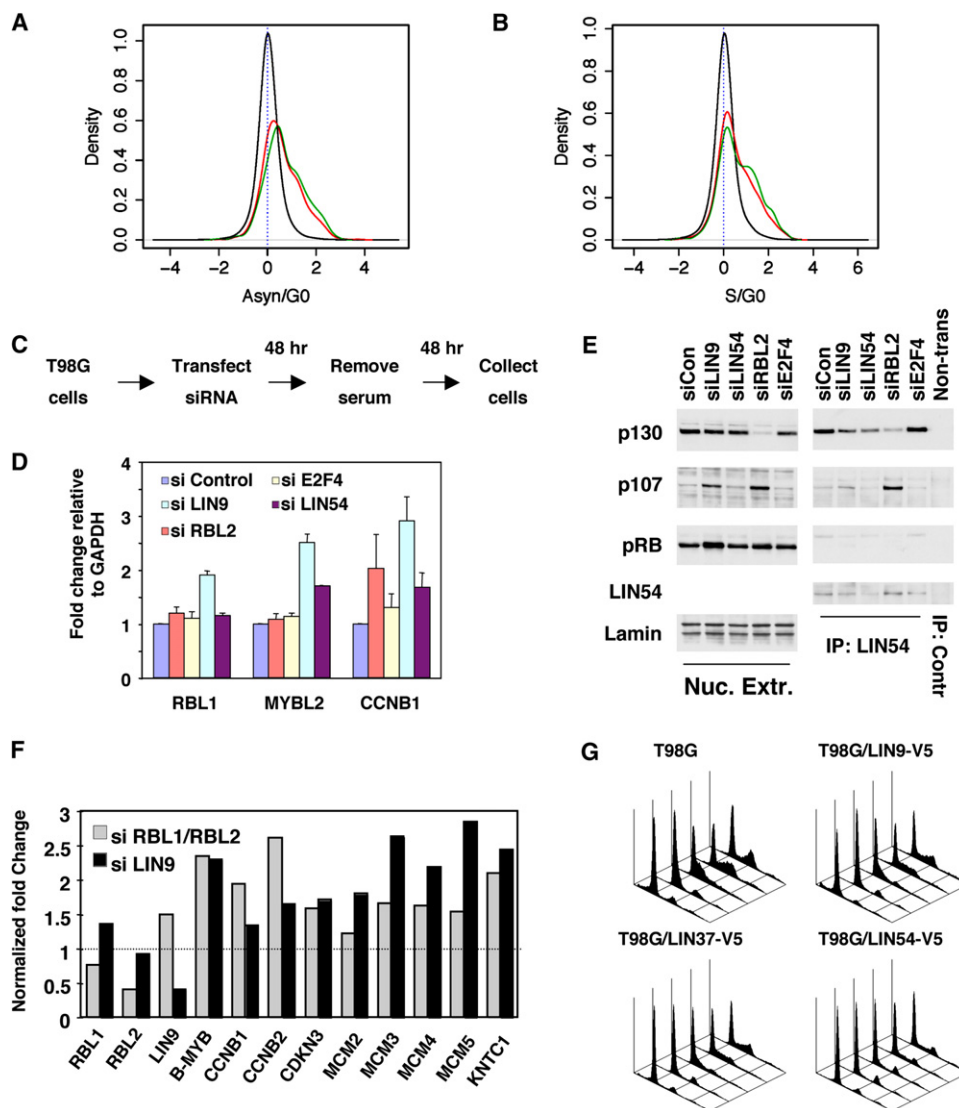


Figure 6. DREAM Complex Represses Cell Cycle-Regulated Genes

(A and B) Global gene expression analysis was performed using T98G cells in asynchronously growing state (Asyn) and after 72 hr of serum starvation (G0, in [A]) or after serum restimulation (S, in [B]). Graphs show the distribution of \log_2 differential gene expression between the indicated series. Black curve represents all the genes present in the microarray, red curve shows genes whose promoters are bound by LIN9, p130, and E2F4 at G0 phase, and green curve shows genes bound by these three factors and LIN54.

(C) Experimental protocol for siRNA-mediated knockdown of DREAM subunits.

(D) RNA isolated from siRNA-transfected T98G cells was analyzed by coupled reverse transcriptase (RT)-qPCR with specific primers. The fold change was calculated relative to GAPDH mRNA levels. Average values and standard deviations for three independent experiments are shown.

(E) T98G cells were treated as in (C), and the expression of RB family proteins and Lamin A (loading control) was tested by western blots (left). Expression of LIN54 and the presence of RB proteins were tested in anti-LIN54 IPs by western blots (right). The left and right panels for each RB protein were developed together with the same exposure time. IP from intact cell extract with unrelated antibody serves as a control.

(F) qPCR was performed using commercial PCR array with gene-specific primers. The mRNA levels of the tested genes upon the depletion of LIN9 or RBL1/RBL2 are plotted relative to their levels in control siRNA-transfected cells. The fold change in each case was calculated relative to the averaged values of several controls (actin, HPRT, RPL13A, GAPDH, and 18S rRNA).

(G) T98G cells and the stable cell lines expressing V5-tagged DREAM subunits were arrested in G0 by confluence and serum starvation for 72 hr and then replated in the presence of serum. The cell-cycle progression of the cells collected at G0 and at 16, 21, 24, and 27 hr poststimulation is shown.

genes while the absence or decreased association of the complex with promoters in S phase correlates with increased expression.

Given the correlation between DREAM complex binding to promoters and repression of target genes, we tested whether the intact DREAM complex was required to

repress gene expression in G0. We depleted the mRNA for *RBL2* (p130), *E2F4*, *LIN9*, and *LIN54* with siRNA, then removed serum to enrich for cells in G0 (Figure 6C). The siRNA transfection of T98G cells resulted in a reduction of mRNA levels of the targeted genes and a corresponding decrease in specific protein levels (Figure S6A and S6B). As shown in Figure 6D, knockdowns of the DREAM subunits had variable effects on the three DREAM target genes tested. The depletion of *LIN9* or *LIN54* was more efficient in upregulating DREAM target gene expression, while the depletion of p130 or *E2F4* had less effect. The loss of an RB-related protein could be compensated by recruitment of their homologs to the complex. Indeed, the knockdown of p130 led to increased expression of the E2F-dependent gene *Rbl1* (p107). Notably, when p130 levels were reduced by RNAi and p107 levels were induced, p107 could be coprecipitated with *LIN54* from the p130-depleted extracts (Figure 6E). Under these conditions, p107 appeared to complement the role of p130 in DREAM and contribute to the repression of target genes. This was confirmed by testing the expression of a panel of DREAM target genes after siRNA knockdown of both p130 and p107. The expression of these genes increased when *LIN9* alone or both p107 and p130 were depleted in G0-arrested cells (Figure 6F). This result supports an active repressor role for the DREAM complex in control of the cell cycle-dependent genes.

Because DREAM complex binds to and represses genes involved in cell-cycle progression, we tested whether ectopic expression of DREAM subunits could affect the cell cycle. T98G cell lines stably overexpressing V5-tagged *LIN9*, *LIN37*, and *LIN54* had a significant delay in progression from the G0 to S phase compared to control cells (Figure 6G). Notably, an independently generated T98G/HAp130 cell line displayed a similar phenotype (Figure S6C). Together with the results presented above, this finding supports a regulatory role for the DREAM complex in mammalian cell cycle progression.

DISCUSSION

Conserved RB/E2F Repressor Complexes Are Present in Different Species

Using a candidate and an unbiased proteomics approach, we identified a specific DNA-binding complex that contains p130, E2F4/5, DP1/2, and five human proteins homologous to products of the *C. elegans* synMuvB group of genes. Similar complexes were previously described in *Drosophila* and *C. elegans* (Harrison et al., 2006; Korenjak et al., 2004; Lewis et al., 2004). The core components of these evolutionarily conserved complexes include an RB-like protein, E2F and DP heterodimer, and RB-binding protein RBBP4 as well as *LIN9*, *LIN37*, *LIN52*, and *LIN54* homologs. Because we found no evidence of interaction between pRB and these synMuvB proteins, it appears that p130 and not pRB serves as the functional ortholog of RB from fly and worm.

The identification of proteins copurifying with p130, *LIN9*, *LIN37*, and *LIN54* revealed a striking consistency in the composition of their respective complexes. The proteomics analysis (Florens and Washburn, 2006) identified the same eight proteins present in complexes associated with all bait proteins. Stoichiometry of the human complex as determined by MudPIT indicates that it is likely comprised of two multiprotein subcomplexes with p130, E2F4/5, and DP1/2 forming one module and the MuvB proteins *LIN9*, *LIN37*, *LIN52*, *LIN54*, and RBBP4 forming a second module. The second module can independently bind to MYB in S phase, and our results indicate that the MYB-MuvB-containing complex does not contain p130, E2F4, or DPs.

The current view proposes that RB proteins serve to recruit chromatin-modifying enzymes to E2F-dependent promoters to impose transcriptional repression of cell-cycle genes. There have been several reports on the interaction between RB family proteins and SIN3/HDAC complex subunits as well as other chromatin-modifying enzymes (references in Frolov and Dyson [2004]). We did not detect any additional components of the DREAM complex such as chromatin-modifying enzymes. Consistent with these findings, a physical interaction between the worm DRM subunits and the nematode histone deacetylase homologs was not observed although *Hda-1 HDAC* is a synMuvB gene (Harrison et al., 2006). Despite the lack of evidence for physical interaction between chromatin modifiers and the DREAM complex in our study, an extensive literature supports a functional interaction. In *C. elegans*, components of NuRD complex belong to synMuvB or synMuvA classes (Poulin et al., 2005; Solari and Ahlinger, 2000). In mouse cells, the recruitment of HDAC to E2F-dependent promoters requires an intact E2F binding site in a target promoter and depends on p130 and p107, but not on pRB (Rayman et al., 2002). It is possible that DREAM subunit RBBP4 serves as a link to recruit chromatin modifiers to the DREAM-targeted promoters because it is a component of both NuRD and SIN3 complexes (Wolffe et al., 2000).

RB Family and DREAM

We observed that p130, but not pRB or p107, was associated with the DREAM complex in G0-arrested cells. This new finding is important for understanding of RB family function because p130 is the predominant RB family protein bound to E2F4- and E2F-regulated promoters in quiescent cells (Balciunaite et al., 2005; Smith et al., 1996). It is possible that p107 or even pRB may be recruited into the DREAM complex under certain conditions, given that prior reports indicated an in vitro interaction of all human RB-like proteins with DREAM subunits (Korenjak et al., 2004) as well as in vivo binding of pRB with *LIN9* in human mesenchymal stem cells (Gagrica et al., 2004). Although expression of p107 increases in S phase when p130 levels are low (Smith et al., 1996), only a small fraction of p107 was bound to *LIN37* in the S phase cells (data not shown). However, when p130 was depleted by siRNA knockdown

in G0-arrested cells we observed both increased expression and binding of p107 to LIN54, indicating that binding of p107 to DREAM subunits could occur when p130 expression is low. Because p107 can bind E2F4, the p107-containing DREAM complex could bind to E2F-dependent promoters and repress cell cycle-dependent genes in the absence of p130. This is consistent with the observation that mammalian p130 and p107 proteins are fully redundant in embryonic development and cell-cycle control while pRb apparently plays a more unique role (reviewed in [Cobrinik \[2005\]](#)).

DREAM Complex Binds to Promoters of Cell Cycle-Regulated Genes in G0

The p130/E2F4 complex has been previously shown to bind to promoters of cell cycle-dependent genes ([Cam et al., 2004](#)). In this report, ChIP and global location analysis for LIN9, LIN54, E2F4, and p130 revealed that the DREAM complex was bound to more than 800 human promoters that included most of the previously reported p130/E2F4 targets. This report extends the previous model by demonstrating that p130 and DP/E2F4 bind to E2F target promoters in G0 as a part of a larger protein complex that also includes RBBP4, LIN9, LIN37, LIN52, and LIN54. We found a remarkably strong correlation of promoter binding between p130/E2F4 with LIN9 and LIN54 that was significantly higher in G0-arrested cells than in S phase cells. Because all target promoters were bound more strongly in G0 compared to S phase, it is likely that DREAM complex is tightly bound to E2F-regulated promoters in G0 and dissociates from these promoters in S phase. Some subunits of the DREAM complex can also interact specifically with MYB ([Osterloh et al., 2007](#); [Pilkinton et al., 2006](#); and this article) and may be involved in expression of MYB-dependent genes important into the G2/M progression. However, we did not observe an enrichment of specific promoters strongly bound by LIN9 and LIN54 in the absence of p130 and E2F4 binding, both in G0 and in S phase cells, although it is possible that a LIN9-LIN54 complex could bind to regions outside the promoters analyzed in our experiments. For example, dMyb, Mip130/LIN9, and Mip120/LIN54 have been implicated in site-specific replication-mediated gene amplification in *Drosophila* ([Beall et al., 2002, 2004](#)). Further studies are required to determine whether the DREAM complex participates in the control of DNA replication or any other additional activities.

A detailed analysis of all promoters in the regions bound by any two DREAM subunits in G0 revealed a strong enrichment for the E2F consensus binding site. This enrichment was also clearly detected when sites bound by LIN9, LIN54, p130, and E2F4 were analyzed individually, supporting the conclusion that these proteins bind as a complex to promoters with a high occurrence of sequences matching the E2F binding site. Previous *in silico* analysis of promoters of human cell cycle-regulated genes established a significant enrichment of the E2F, NRF1, NF-Y, and CREB binding motifs in their promoters ([Elkon et al.,](#)

[2003](#)). Using a global location analysis, we found that DREAM complex bound to a similarly enriched (with the exception of NF-Y) group of promoters. The enrichment of E2F and NRF1 motifs was also reported in the smaller subset of p130- and E2F4-bound promoters ([Cam et al., 2004](#)). In our analysis, these motifs were present in regions with highest binding ranks that were most likely bound by all four DREAM subunits tested. Together, these results indicate that the majority of the cell cycle-regulated genes contain E2F consensus motifs in their promoters and even those genes that do not have an obvious E2F binding site in their promoters were bound by the E2F4-containing DREAM complex. These findings also suggest that E2Fs could cooperate with other transcription factors in regulation of cell cycle-dependent genes.

Genes Regulated by the DREAM Complex

Gene ontology analysis of DREAM-bound promoters revealed a predominant enrichment for cell cycle and related functional categories. This result is in agreement with the previous model for the functional role of p130/E2F4 in the regulation of cell cycle-dependent genes. We did not observe a significant enrichment for genes involved in development. This finding distinguishes the human complex from its *Drosophila* and *C. elegans* orthologs that have been shown to regulate development and cell fate specification ([Fay and Han, 2000](#); [Korenjak et al., 2004](#)). A broader role in transcriptional repression and cell-cycle control has been demonstrated for some, but not all, DREAM subunits, including E2F, DP, RBBP4, LIN9, and RB orthologs in flies and worms ([Boxem and van den Heuvel, 2002](#); [Dimova et al., 2003](#); [Poulin et al., 2005](#); [Taylor-Harding et al., 2004](#)).

The expression analysis of DREAM target genes supports their role in cell-cycle control because the majority of these genes were repressed in G0 and induced upon S phase entry. Significantly, the DREAM complex not only binds to the promoters of cell cycle-regulated genes in the repressed state but also serves to actively repress these genes. Consistently, we observed that the ectopic expression of DREAM subunits, including p130 in T98G cells, results in a significantly delayed reentry into the cell cycle after G0 growth arrest. Because p130 has been previously shown to be the predominant RB family protein in E2F4 repressor complexes in quiescent cells, our finding significantly extends the understanding of the molecular mechanism of regulation of the cell cycle-dependent gene expression.

Conclusion

A systematic analysis integrating proteomics, genomics, and bioinformatics resulted in the identification of a conserved p130/E2F4-containing protein complex in human cells that functions as a transcriptional repressor of cell cycle-dependent genes. A complete understanding of the RB family function will await similarly designed studies of other RB family members and E2Fs in a variety of experimental systems, including differentiation and oncogenic

transformation models as well as specialized tissues in the organism. Our study significantly expands knowledge of the global control of cell-cycle gene expression and validates the benefit of an integrated experimental approach to study the function of multisubunit DNA-binding protein complexes.

EXPERIMENTAL PROCEDURES

Cell Lines, siRNA, and Antibodies

Human glioblastoma T98G cells and primary human LF1 fibroblasts were from ATCC. T98G and T98G/HAp130 cells were synchronized in G0 and S phase by serum starvation and restimulation as described (Litovchick et al., 2004). Stable T98G-based cell lines expressing V5-tagged human LIN9, LIN37, LIN52, and LIN54 were generated using retroviral gene transfer (Supplemental Data). For the siRNA-mediated depletion, SMARTpool siRNA pools (Dharmacon) were transfected using TransIT-siQUEST reagent (Mirus Bio) according to the manufacturer's protocol. Rabbit antibodies specific to human p130, RBBP4, LIN9, LIN37, LIN52, and LIN54 were raised against peptide epitopes derived from predicted protein sequences (Bethyl). Commercial antibodies used in this study are listed in the Supplemental Data section.

MudPIT

HAp130 was isolated from T98G/HAp130 cells, and endogenous p130 was isolated from T98G or from T98G/HAp130 cells. LIN9, LIN37, and LIN54 were isolated from T98G-based cell lines expressing V5-tagged proteins. Approximately 200 mg of cell extracts were incubated overnight at 4°C with 1 µg/ml of specific anti-peptide antibody (Bethyl) and 50 µl of protein A beads, or with 2 µg/ml of anti-HA matrix for HAp130 (Pierce). IPs from parental T98G cells using 2 µg/ml of anti-HA matrix (Pierce), 1 µg/ml of rabbit anti-HA (Santa Cruz Biotech), or anti-V5 (Bethyl) antibodies were used as controls. After washing, beads were incubated with 200 µg/ml of the corresponding peptide to elute the complexes that were then analyzed by MudPIT as described in Florens and Washburn (2006) and the Supplemental Data section.

Chromatin Immunoprecipitation

Chromatin immunoprecipitation (ChIP) was performed as described before (Rayman et al., 2002). PCR primer sequences are available upon request. For ChIP-chip, ChIP DNA was amplified using a ligation-mediated PCR, labeled with biotin as described in Carroll et al. (2006), and hybridized to an Affymetrix human promoter array 1.0 R.

Quantitative PCR and Gene Expression Analysis

All quantitative PCRs (qPCRs) were performed using SYBR green. For ChIP-qPCR, serial dilutions of the input genomic DNA were included with each series and used to calculate the specific ChIP enrichments as a percent of input DNA as described in Papp and Muller (2006). For expression analysis, total RNA was isolated using TRIzol reagent (Invitrogen) and purified using RNAeasy kit (QIAGEN). For qPCR analysis, RNA was reverse transcribed using the Superscript III RT (Invitrogen) and used as a template for PCR with in-house primers or Cell Cycle RT² PCR Array (SuperArray Bio. Corp.). The fold change of a specific mRNA was calculated relative to controls using the 2^{-ΔΔCt} method. Sequences of PCR primers are available upon request.

Microarray Gene Expression Analysis

RNA was purified from T98G cells that were either cycling, G0 arrested, or released into S phase for 10 hr and 16 hr. For each experimental condition, 15 µg of RNA was processed and hybridized against Affymetrix GeneChip Human Genome U133 Plus 2.0 Array.

Computational Analysis

Tiling array analysis algorithm MAT (Johnson et al., 2006) was applied to each factor's triplicate ChIP-chip data to determine binding sites

using a bandwidth of 300 bp and p value cutoff of 10⁻⁵. Binding sites were assigned MAT scores reflecting the ChIP-chip fold enrichment. Two factors were considered to bind to the same site if the chromosome coordinates of the binding sites in human genome assembly (version Hg18) overlapped. Annotation of binding sites, RefSeq mapping, and motif finding were performed using the CEAS server at <http://ceas.cbi.pku.edu.cn> (Ji et al., 2006). Gene ontology analysis was conducted using DAVID at <http://david.abcc.ncifcrf.gov/> using default parameters (Dennis et al., 2003). Gene expression microarray data on asynchronous T98G cells and cells in G0 or S phase (combined 10 hr and 16 hr poststimulation data sets) were summarized by RMA (Irizarry et al., 2003) using an optimized probe mapping (Dai et al., 2005). Differential gene expression was calculated based on average fold change.

Supplemental Data

Supplemental Data include six figures, five tables, Supplemental Experimental Procedures, and Supplemental References and can be found with this article online at <http://www.molecule.org/cgi/content/full/26/4/539/DC1>.

ACKNOWLEDGMENTS

This work was funded in part by Public Health Service grants PO1 CA50661 and RO1 CA063113 (J.A.D.), HG004069-01 (X.S.L. and X.Z.), and Claudia Adams Barr Award for Cancer Research (L.L.). We thank N. Lents and B. Dynlacht for ChIP protocol and PCR primer sequences, S. Gaubatz for sharing unpublished results, and N. Dyson and C. Ceol for discussions. We acknowledge R. Toddings and K. Kashin for excellent technical assistance. V. Kashin provided initial computational analysis of the ChIP-chip data.

Received: December 28, 2006

Revised: March 12, 2007

Accepted: April 20, 2007

Published: May 24, 2007

REFERENCES

- Balciunaite, E., Spektor, A., Lents, N.H., Cam, H., Te Riele, H., Scime, A., Rudnicki, M.A., Young, R., and Dynlacht, B.D. (2005). Pocket protein complexes are recruited to distinct targets in quiescent and proliferating cells. *Mol. Cell. Biol.* 25, 8166–8178.
- Beall, E.L., Manak, J.R., Zhou, S., Bell, M., Lipsick, J.S., and Botchan, M.R. (2002). Role for a Drosophila Myb-containing protein complex in site-specific DNA replication. *Nature* 420, 833–837.
- Beall, E.L., Bell, M., Georgette, D., and Botchan, M.R. (2004). Dm-myb mutant lethality in Drosophila is dependent upon mip130: positive and negative regulation of DNA replication. *Genes Dev.* 18, 1667–1680.
- Boxem, M., and van den Heuvel, S. (2002). C. elegans class B synthetic multivulva genes act in G(1) regulation. *Curr. Biol.* 12, 906–911.
- Cam, H., Balciunaite, E., Blais, A., Spektor, A., Scarpulla, R.C., Young, R., Kluger, Y., and Dynlacht, B.D. (2004). A common set of gene regulatory networks links metabolism and growth inhibition. *Mol. Cell* 16, 399–411.
- Carroll, J.S., Meyer, C.A., Song, J., Li, W., Geistlinger, T.R., Eeckhoutte, J., Brodsky, A.S., Keeton, E.K., Fertuck, K.C., Hall, G.F., et al. (2006). Genome-wide analysis of estrogen receptor binding sites. *Nat. Genet.* 38, 1289–1297.
- Ceol, C.J., Stegmeier, F., Harrison, M.M., and Horvitz, H.R. (2006). Identification and classification of genes that act antagonistically to let-60 Ras signaling in Caenorhabditis elegans vulval development. *Genetics* 173, 709–726.
- Classon, M., and Dyson, N. (2001). p107 and p130: versatile proteins with interesting pockets. *Exp. Cell Res.* 264, 135–147.

- Classon, M., and Harlow, E. (2002). The retinoblastoma tumour suppressor in development and cancer. *Nat. Rev. Cancer* 2, 910–917.
- Cobrinik, D. (2005). Pocket proteins and cell cycle control. *Oncogene* 24, 2796–2809.
- Dai, M., Wang, P., Boyd, A.D., Kostov, G., Athey, B., Jones, E.G., Bunney, W.E., Myers, R.M., Speed, T.P., Akil, H., et al. (2005). Evolving gene/transcript definitions significantly alter the interpretation of GeneChip data. *Nucleic Acids Res.* 33, e175.
- Dennis, G., Jr., Sherman, B.T., Hosack, D.A., Yang, J., Gao, W., Lane, H.C., and Lempicki, R.A. (2003). DAVID: Database for Annotation, Visualization, and Integrated Discovery. *Genome Biol.* 4, P3.
- Dimova, D.K., and Dyson, N.J. (2005). The E2F transcriptional network: old acquaintances with new faces. *Oncogene* 24, 2810–2826.
- Dimova, D.K., Stevaux, O., Frolov, M.V., and Dyson, N.J. (2003). Cell cycle-dependent and cell cycle-independent control of transcription by the Drosophila E2F/RB pathway. *Genes Dev.* 17, 2308–2320.
- Elkon, R., Linhart, C., Sharan, R., Shamir, R., and Shiloh, Y. (2003). Genome-wide in silico identification of transcriptional regulators controlling the cell cycle in human cells. *Genome Res.* 13, 773–780.
- Fay, D.S., and Han, M. (2000). The synthetic multivulval genes of *C. elegans*: functional redundancy, Ras-antagonism, and cell fate determination. *Genesis* 26, 279–284.
- Florens, L., and Washburn, M.P. (2006). Proteomic analysis by multidimensional protein identification technology. *Methods Mol. Biol.* 328, 159–175.
- Florens, L., Carozza, M.J., Swanson, S.K., Fournier, M., Coleman, M.K., Workman, J.L., and Washburn, M.P. (2006). Analyzing chromatin remodeling complexes using shotgun proteomics and normalized spectral abundance factors. *Methods* 40, 303–311.
- Frolov, M.V., and Dyson, N.J. (2004). Molecular mechanisms of E2F-dependent activation and pRB-mediated repression. *J. Cell Sci.* 117, 2173–2181.
- Gagrica, S., Hauser, S., Kofschoten, I., Osterloh, L., Agami, R., and Gaubatz, S. (2004). Inhibition of oncogenic transformation by mammalian Lin-9, a pRB-associated protein. *EMBO J.* 23, 4627–4638.
- Harrison, M.M., Ceol, C.J., Lu, X., and Horvitz, H.R. (2006). Some *C. elegans* class B synthetic multivulva proteins encode a conserved LIN-35 Rb-containing complex distinct from a NuRD-like complex. *Proc. Natl. Acad. Sci. USA* 103, 16782–16787.
- Irizarry, R.A., Hobbs, B., Collin, F., Beazer-Barclay, Y.D., Antonellis, K.J., Scherf, U., and Speed, T.P. (2003). Exploration, normalization, and summaries of high density oligonucleotide array probe level data. *Biostatistics* 4, 249–264.
- Ji, X., Li, W., Song, J., Wei, L., and Liu, X.S. (2006). CEAS: cis-regulatory element annotation system. *Nucleic Acids Res.* 34, W551–W554.
- Johnson, W.E., Li, W., Meyer, C.A., Gottardo, R., Carroll, J.S., Brown, M., and Liu, X.S. (2006). Model-based analysis of tiling-arrays for ChIP-chip. *Proc. Natl. Acad. Sci. USA* 103, 12457–12462.
- Korenjak, M., Taylor-Harding, B., Binne, U.K., Satterlee, J.S., Stevaux, O., Aasland, R., White-Cooper, H., Dyson, N., and Brehm, A. (2004). Native E2F/RBF complexes contain Myb-interacting proteins and repress transcription of developmentally controlled E2F target genes. *Cell* 119, 181–193.
- Lewis, P.W., Beall, E.L., Fleischer, T.C., Georlette, D., Link, A.J., and Botchan, M.R. (2004). Identification of a Drosophila Myb-E2F2/RBF transcriptional repressor complex. *Genes Dev.* 18, 2929–2940.
- Litovchick, L., Chestukhin, A., and DeCaprio, J.A. (2004). Glycogen synthase kinase 3 phosphorylates RBL2/p130 during quiescence. *Mol. Cell. Biol.* 24, 8970–8980.
- Osterloh, L., Von Eyss, B., Schmit, F., Rein, L., Hubner, D., Samans, B., Hauser, S., and Gaubatz, S. (2007). The human synMuv-like protein LIN-9 is required for transcription of G2/M genes and for entry into mitosis. *EMBO J.* 26, 144–157.
- Papp, B., and Muller, J. (2006). Histone trimethylation and the maintenance of transcriptional ON and OFF states by trxG and PcG proteins. *Genes Dev.* 20, 2041–2054.
- Payton, M., and Coats, S. (2002). Cyclin E2, the cycle continues. *Int. J. Biochem. Cell Biol.* 34, 315–320.
- Pilkinton, M., Sandoval, R., Song, J., Ness, S.A., and Colamonici, O.R. (2006). Mip/LIN-9 regulates the expression of B-MYB, and the induction of cyclin a, cyclin B and CDK1. *J. Biol. Chem.* 282, 168–175.
- Poulin, G., Dong, Y., Fraser, A.G., Hopper, N.A., and Ahringer, J. (2005). Chromatin regulation and sumoylation in the inhibition of Ras-induced vulval development in *Caenorhabditis elegans*. *EMBO J.* 24, 2613–2623.
- Rayman, J.B., Takahashi, Y., Indjeian, V.B., Dannenberg, J.H., Catchpole, S., Watson, R.J., te Riele, H., and Dynlacht, B.D. (2002). E2F mediates cell cycle-dependent transcriptional repression in vivo by recruitment of an HDAC1/mSin3B corepressor complex. *Genes Dev.* 16, 933–947.
- Ren, B., Cam, H., Takahashi, Y., Volkert, T., Terragni, J., Young, R.A., and Dynlacht, B.D. (2002). E2F integrates cell cycle progression with DNA repair, replication, and G2/M checkpoints. *Genes Dev.* 16, 245–256.
- Smith, E.J., Leone, G., DeGregori, J., Jakoi, L., and Nevins, J.R. (1996). The accumulation of an E2F-p130 transcriptional repressor distinguishes a G0 cell state from a G1 cell state. *Mol. Cell. Biol.* 16, 6965–6976.
- Solari, F., and Ahringer, J. (2000). NURD-complex genes antagonise Ras-induced vulval development in *Caenorhabditis elegans*. *Curr. Biol.* 10, 223–226.
- Taylor-Harding, B., Binne, U.K., Korenjak, M., Brehm, A., and Dyson, N.J. (2004). p55, the Drosophila ortholog of RbAp46/RbAp48, is required for the repression of dE2F2/RBF-regulated genes. *Mol. Cell. Biol.* 24, 9124–9136.
- Wikenheiser-Brokamp, K.A. (2006). Retinoblastoma family proteins: insights gained through genetic manipulation of mice. *Cell. Mol. Life Sci.* 63, 767–780.
- Wolffe, A.P., Urnov, F.D., and Guschin, D. (2000). Co-repressor complexes and remodelling chromatin for repression. *Biochem. Soc. Trans.* 28, 379–386.

Accession Numbers

The GEO database accession number for the ChIP-chip data reported in this paper is GSE7516.